References

AITKEN, D. W., BERON, B. L., YENICAY, G. & ZULLINGER, H. R. (1967). IEEE *Trans. Nucl. Sci.* **NS-14**, 468.

BARTUNIK, H. D. & BORCHERT, T. (1989). *Acta Cryst.* A**45**, 718–726.

BARU, S. E., PROVIZ, G. I., SAVINOV, G. A., SIDOROV, V. A., KHABAKHSHEV, A. G., SHUVALOV, B. N. & YAKOVLEV, V. A. (1978). *Nucl. Instrum. Methods*, **152**, 209–212.

BURZLAFF, H. & GRUBE, H.-H. (1980). *Z. Kristallogr.* **152**, 83–93.

BURZLAFF, H., LANGE, J. & ROTHAMMEL, W. (1987). *Acta Cryst.* A**43**, C267.

CRUICKSHANK, D. W. J., HELLIWELL, J. R. & MOFFAT, K. (1987). *Acta Cryst.* A**43**, 656–674.

GOMM, M. (1993). *Crystallographic Computing* 6, pp. 6–9. IUCr/Oxford Univ. Press.

HELLIWELL, J. R. (1992). *Macromolecular Crystallography with Synchrotron Radiation*, pp. 297–298. Cambridge Univ. Press.

International Tables for Crystallography (1992). Vol. C, edited by A. J. C. WILSON, pp. 538–555. Dordrecht/Boston/London: Kluwer Academic Publishers.

International Tables for X-ray Crystallography (1959). Vol. II, edited by J. S KASPER & K. LONSDALE, p. 330, equation (6). Birmingham: Kynoch Press. (Present distributor Kluwer Academic Publishers, Dordrecht.)

International Tables for X-ray Crystallography (1962). Vol. III, edited by C. H. MACGILLAVRY, G. D. RIECK & K. LONSDALE, pp. 152, 153. Birmingham: Kynoch Press. (Present distributor Kluwer Academic Publishers, Dordrecht.)

KAELBLE, E. F. (1967). *Handbook of X-rays*, pp. 3-1, 3-2, 3-27. New York: McGraw-Hill.

KRAMERS, H. A. (1923). *Philos. Mag.* **46**, 836–871.

LANGE, J. (1995). *Acta Cryst.* A**51**, 559–565.

LANGE, J. & BURZLAFF, H. (1991*a*). *J. Appl. Cryst.* **24**, 190–193.

LANGE, J. & BURZLAFF, H. (1991*b*). *J. Appl. Cryst.* **24**, 1060–1062.

LANGE, J. & BURZLAFF, H. (1992). *J. Appl. Cryst.* **25**, 440–443.

LARSON, A. C. (1970). *Crystallographic Computing*, p. 292, equation (22). Copenhagen: Munksgaard.

MIYAHARA, J., TAKAHASHI, K., AMEMIYA, Y., KAMIYA, N. & SATOW, Y. (1986). *Nucl. Instrum. Methods*, A**246**, 572–578.

RABINOVICH, D. & LOURIE, B. (1987). *Acta Cryst.* A**43**, 774–780.

SAKAMAKI, T., HOSOYA, S. & FUKAMACHI, T. (1980). *J. Appl. Cryst.* **13**, 433–437.

Acta Cryst. (1995). A**51**, 936–942

A New Quasiperiodic Tiling with Dodecagonal Symmetry

BY YASUNARI WATANABE AND TAKASHI SOMA

The Institute of Physical and Chemical Research, Wako-shi, Saitama 351-01 *Japan*

AND MASAHISA ITO

Department of Material Science, Faculty of Science, Himeji Institute of Technology, Kamigori, Ako-gun, Hyogo 678-12 *Japan*

(*Received* 7 *July* 1994; *accepted* 4 *July* 1995)

Abstract

A new quasiperiodic (QP) pattern with dodecagonal symmetry defined by a self-similar inflation/deflation rule is presented. The pattern consists of three kinds of base tiles, thin rhombus, regular triangle and square, and their self-similar inflation/deflation rule is shown to be derived from a regular zonogon with 12-fold symmetry. The self-similar transformation matrix for this pattern is derived and the quasiperiodicity is discussed.

1. Introduction

The properties of quasiperiodic tilings with dodecagonal symmetry have been discussed by several authors. The studies of quasiperiodic tilings with pentagonal and decagonal symmetry began with the discovery of Al–Mn (icosahedral phase) (Schechtman, Blech, Gratias & Cahn, 1984) and Al–Fe (decagonal phase) quasicrystals (Fung *et al.*, 1986). The structure of crystalline states with dodecagonal symmetry in the Ni–Cr amorphous phase (Ishimasa, Nissen & Fukano, 1985) gives clues to studies of quasicrystal modeling. A dodecagonal quasiperiodic tiling (DQPT) was first presented by the grid method and self-similar inflation (Stampfli, 1986), which contains regular triangles, squares and rhombi. Another approach for DQPT was proposed using a projection method (Yang & Wei, 1987). The projection and grid methods have been extended and generalized with 3-, 4-, 5-, 6-, 8- and 12-fold symmetry (Whittaker & Whittaker 1988; Socolar, 1989) and algebraic studies of dodecagonal tiling have been carried out in detail (Niizeki & Mitani, 1987). Recently, octagonal, decagonal and dodecagonal tilings have been summarized in relation to Amman bar grids (Lück, 1993). In this paper, a new DQPT is presented, which is characterized by a matching self-similar inflation/deflation rule in building self-similarity. The quasiperiodicity is verified by the fact that the ratios of numbers of constituent base tiles (regular triangle, square and rhombus) converge to an irrational number when the infinite iteration of the inflation is operated on each tile.

2. Generation of DQPT

It is shown that the self-similar inflation rule for DQPT is derived from a regular zonogon (RZ) with 12-fold rotational symmetry consisting of three types of rhombi (thin and thick rhombus, and square), as shown in Fig. 1(*c*). Consider the inflated rhombi of the first generation with an inflation ratio of $2+3^{1/2}$ based on this RZ pattern: a thin rhombus including a $\pi/6$ sector at the center and the symmetric pattern with respect to the peripheral thin rhombus; a thick rhombus including a $2\pi/3$ sector at the center; a square including a $\pi/2$ sector at the center and four thick half rhombi added outside the peripheral thin rhombus (Fig. 1*c*).

Split the thick rhombus into two regular triangles and consider the triangle as one of the base tiles. Modify the edges of length $2+3^{1/2}$ for the inflated thin rhombus, triangle and square into a zigzag shape so that all of the edges match as shown in Fig. 6. From the symmetry of inflated tiles, it is shown that the first generation of regular triangle and square have point group C_s and the rhombus has point group C_{2v}. The zigzag-shaped rhombus, triangle and square have point symmetry C_2, C_3 and C_4, respectively. Because of the discrepancy in the symmetry of the base-tile patterns in the inflated

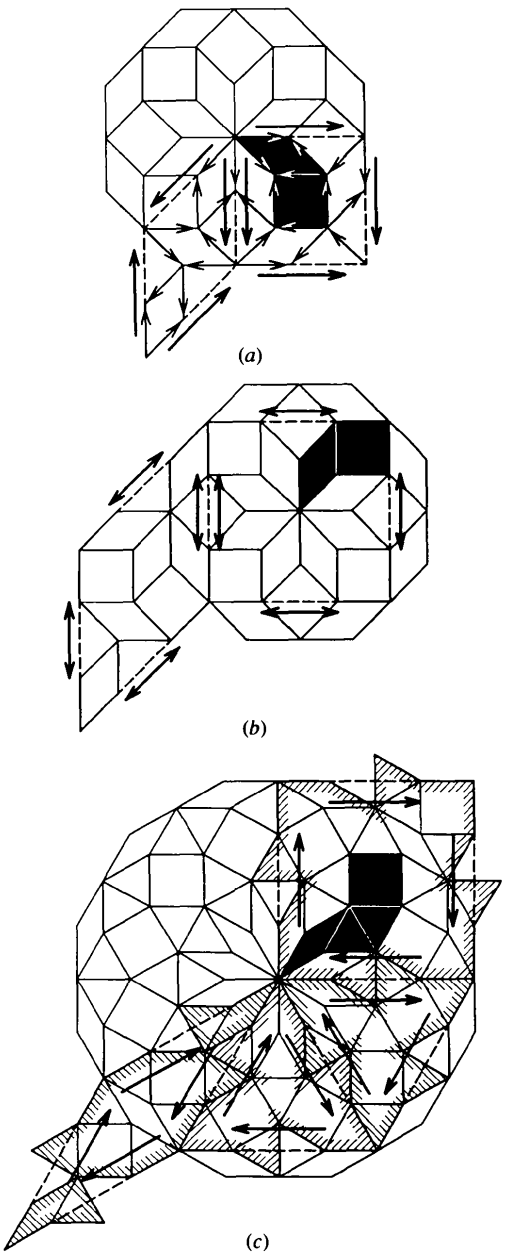

Fig. 1. The 2D matching rule of the inflation with arrow notation on the edge. Black tiles show the zeroth-generation base tile. (*a*) Polar case of the first octagonal pattern generated by partitioning RZ into inflated rhombus and square tiles. (*b*) Nonpolar case of the second octagonal pattern. (*c*) Polar case of the dodecagonal pattern generated by partitioning RZ into inflated rhombus, regular triangle and square tiles drawn with zigzag edge. Arrows on the edges of the base tiles are abbreviated.

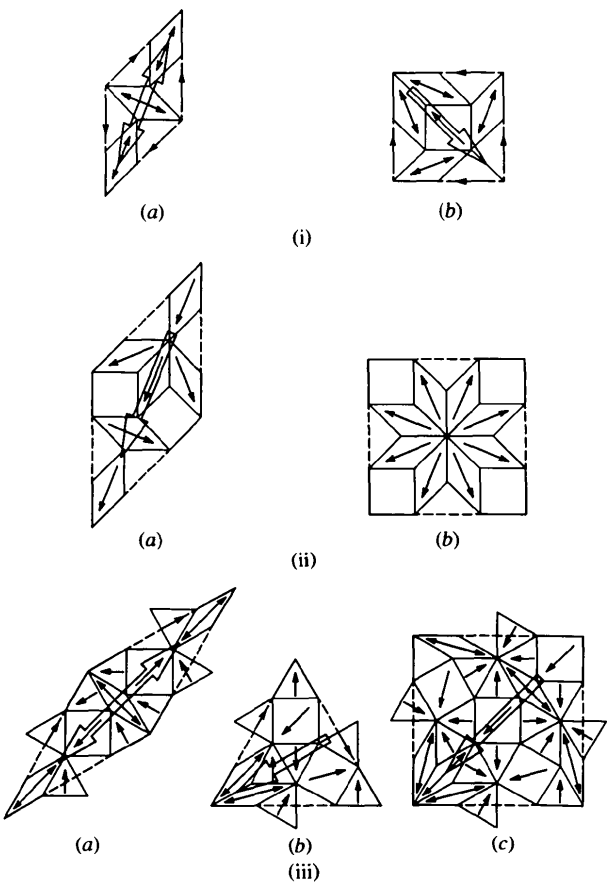

Fig. 2. (i) Definiton of orientation of inflated tiles of the first octagonal tile. (*a*) Inflated rhombus and (*b*) square tiles with small orientational arrow on the base tile. The large arrow represents the orientation of (*a*) rhombus and (*b*) square without the small orientational arrow. (ii) Orientation of inflated second octagonal tiles. (*a*) Inflated rhombus and (*b*) square. Notation of large and small orientational arrows is the same as in (i). Double-headed arrows on the base tiles are abbreviated. (iii) Orientation of inflated dodecagonal tiles. (*a*) Inflated rhombus, (*b*) regular triangle and (*c*) square. Notation of large and small orientational arrows is the same as in (i).

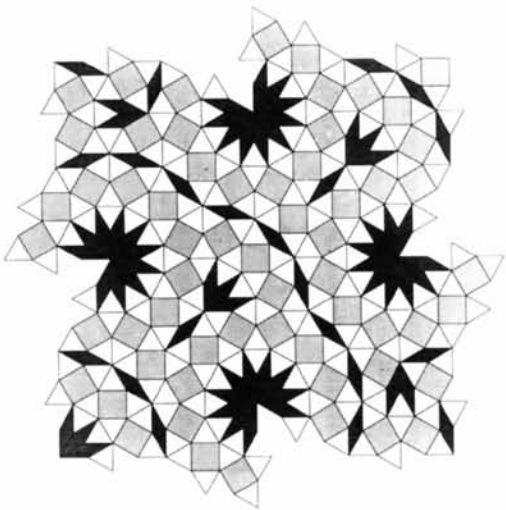

(*a*)

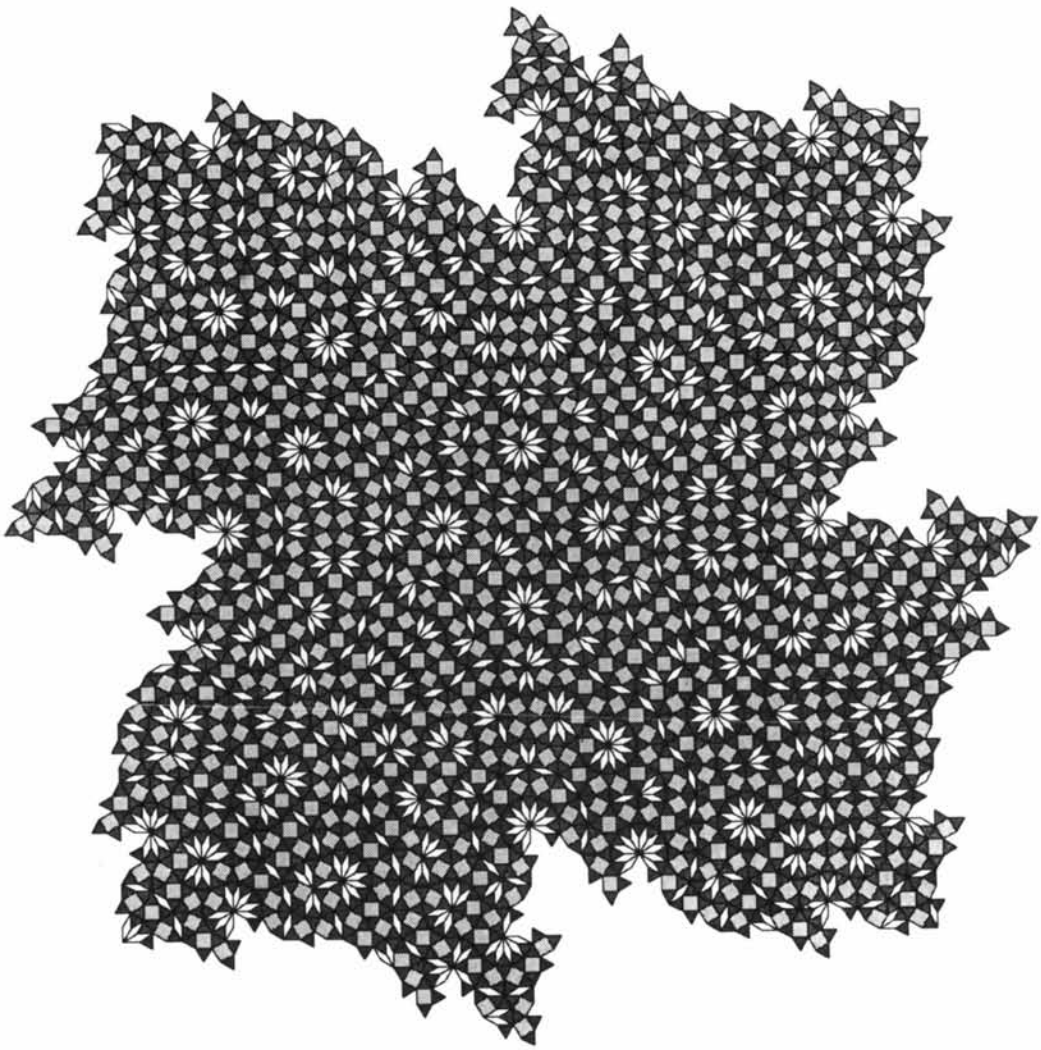

(*b*)

Fig. 3. (*a*) Second and (*b*) third inflated square tile generated by deflation of second square tile (*a*).

patterns and the patterns themselves, it is necessary to specify the orientation of the base tiles in the inflated pattern to define the inflation rule. The orientations of triangles and squares are shown by the arrow on each base tile as in Figs. 2(iii)(*b*) and (*c*).

Since any orientations of the base tile are allowable, every combination of the base-tile orientation in the first-generation pattern defines a different inflation/deflation rule and generates a different self-similar pattern. If different rules are selected randomly in the inflation sequence, a random tiling can be generated in which 12-fold symmetry is broken. This problem will be discussed elsewhere.

The dodecagonal symmetry of these patterns is apparent by considering the 12 thin rhombi as arranged at the center of the RZ. It is easy to show that, by repetition of the inflation operations (magnified by $2+3^{1/2}$ after each assembly), the pattern can cover an area of arbitrary size. This perfect 12-fold symmetry cannot be found in the crystalline symmetry or periodic structure with translational order. The second- or third-generation patterns for a square tile, obtained by the inflation/deflation rule defined in Fig. 2(iii), are shown in Figs. 3(*a*) and (*b*). The second-generation patterns of DQPT by the same inflation/deflation rule having 12-fold symmetry are shown with colored tiles in Fig. 4.

It is interesting to note that the inflation rule for the first octagonal pattern (Beenker, 1982) and the second octagonal pattern (Watanabe, Ito & Soma, 1987) can be derived by patterning based on a RZ of 8-fold symmetry as shown in Figs. 1(*a*) and (*b*).

In order to verify the dodecagonal symmetry, the diffraction pattern of the vertices in the second-generation pattern for the square tile is calculated and shown in Fig. 5. Although most of the strong reflections reveal 12-fold symmetry, weak spots with 4-fold symmetry are noticeable, reflecting the distribution of the lattice vertices of a square tile of only the second generation.

The fractal growth of the circumference of each tile is clear at a glance. The fractal dimension D (Mandelbrot, 1983) is represented by a ratio of logarithmic functions, $\log N/\log(1/r)$, where N is the number of interval units of the generator that corresponds to a Koch curved line and $1/r$ is a straight interval unit. In the case of DQPT, $N=5$ and $r=2+3^{1/2}$ and $D\simeq 1.22$ is obtained by the geometry shown in Fig. 6.

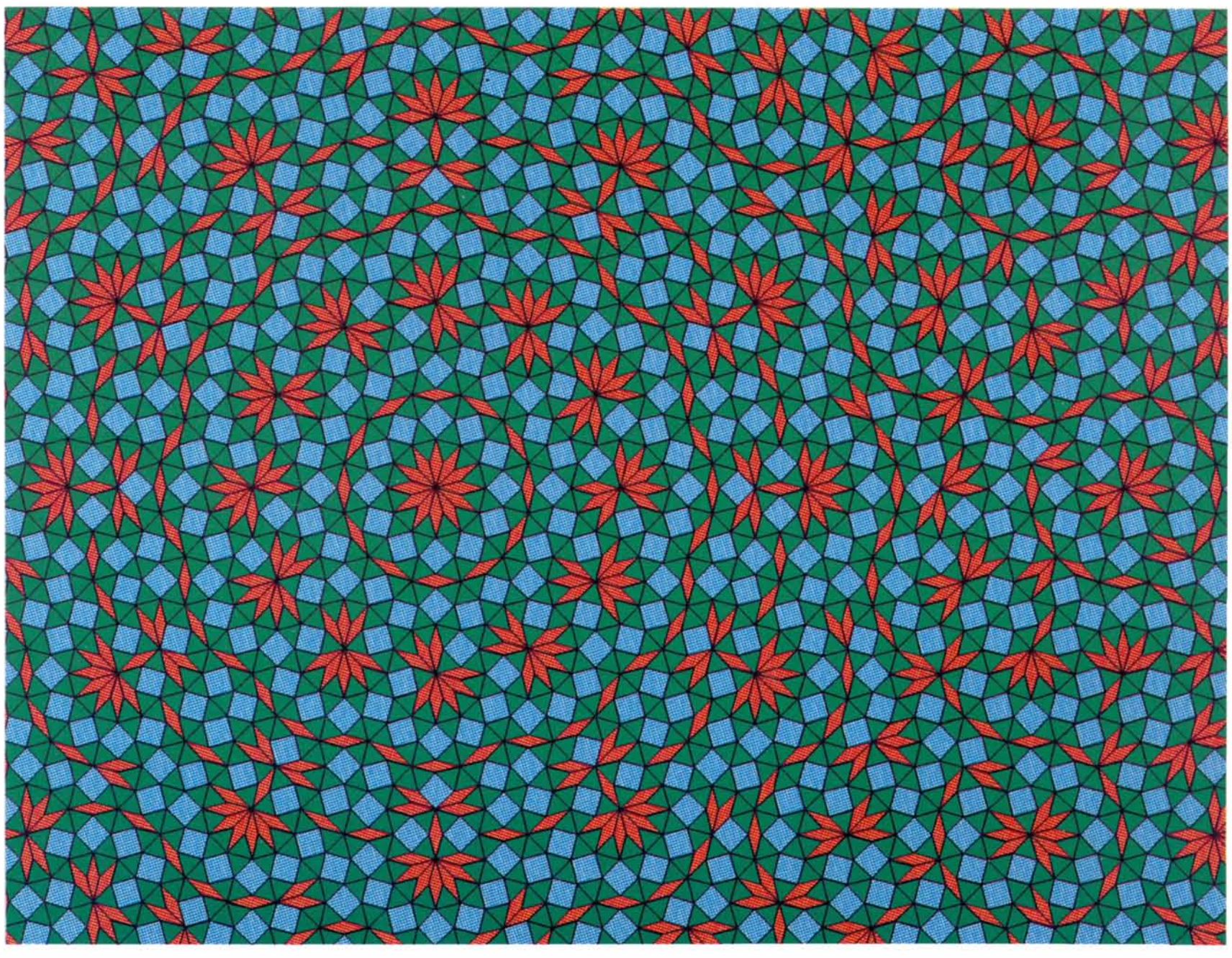

Fig. 4. Third-generation pattern of a DQPT around the center of dodecagonal symmetry. Coloring with orange for rhombus, green for triangle and aqueous blue for square.

3. Matching rule of DQPT

In the building of quasiperiodic tiling, it is necessary to take into account the matching rule in the self-similar inflation of the base tiles. In this section, the relation between the arrow notation on the edge, which is used conventionally as an expression of the rule, and the symmetry of the inflated pattern is considered. If an internal assembly point on an edge shared by adjacent base tiles is asymmetric in the self-similar inflation, as is seen in the shared edge that has polarity with $1:2^{1/2}$ division in the first octagonal tiling and $1:\tau[\tau=(1+5^{1/2})/2]$ division in the pentagonal tiling (de Bruijn, 1981; Watanabe & Ikegami, 1991; Zobetz & Preisinger, 1990; Zobetz, 1992), the sense of the arrow on the edge (usually shown by the arrow notation) has to be consistent with that of the base tile. However, if assembly points exist at a symmetrical position like the $1:2^{1/2}:1$ division in the second octagonal tiling, the common edge is nonpolar. Examples of the edge connection are shown in Figs. 1(*a*) and (*b*) for the first and second octagonal patterns with the sense of the arrow on the edge and no sense of the arrow, respectively.

In the polar case, once the rule of the arrow on the edge is satisfied, a 2D quasi-periodic (QP) pattern is determined uniquely and is automatically generated by the inflation of any order. In the nonpolar case, however, the QP pattern could not be determined uniquely by considering only the matching of the assembly points on the edge. In the DQPT case, although a clockwise arrow notation could be presented for the edges of three kinds of tiles represented by a zigzag boundary (polar case) as in Fig. 1(*c*), where one tile is matched to the adjacent one by a pair of arrows with opposite sense on the common edge, any edge can match every rotation of square and triangle tiles. In order to resolve this ambiguity, the orientation of a base tile in the inflated pattern is considered. An orientational arrow (o.a.) is presented on the base tile according to the symmetry of the inflated pattern as described for the building of the DQPT in the previous section.

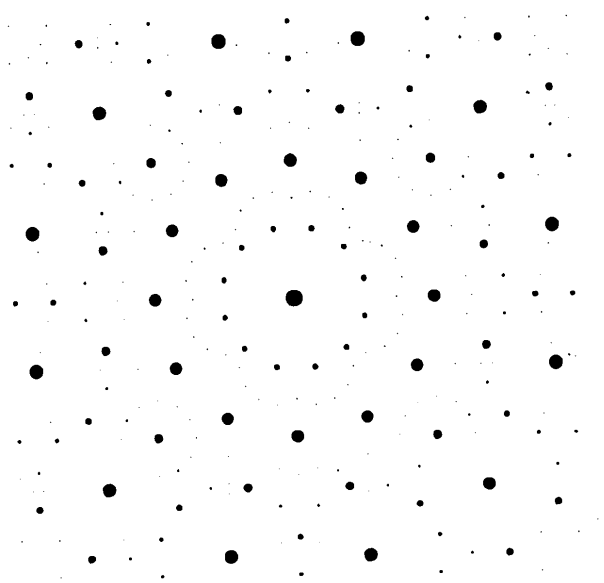

Fig. 5. Simulated diffraction pattern of a second-generation square tile.

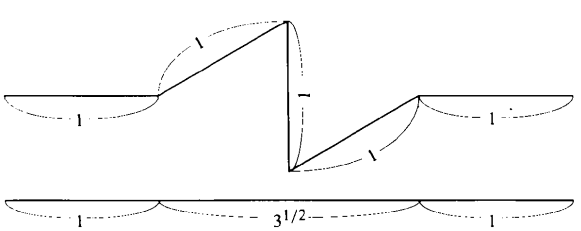

Fig. 6. Geometrical fractal generator of the circumference of DQPT.

The rule is applied to the first and second octagonal tilings. In the first octagonal case, the inflated tiles have C_s and C_{2v} point groups for the square and rhombus, respectively, as shown in Fig. 1(*a*). As the o.a. pattern of the inflated first octagonal rhombus and square take the same point symmetry as base tiles C_{2v} and C_s, respectively, its QP pattern can be determined uniquely as shown in Figs. 2(i)(*a*) and (*b*). The symmetry of the arrow on the edge is consistent with that of the inflated pattern with the o.a. of the base tiles. In the second octagonal case, the inflated rhombus and square have C_s and C_{8v} point groups, respectively, as shown in Fig. 1(*b*). In this case, since the second octagonal rhombus pattern has lower symmetry (C_s) than the first (C_{2v}), its orientation must be defined by a large arrow along the long diagonal line. Therefore, while the point symmetry of the o.a. pattern in the inflated square, C_{8v}, is conserved as in Fig. 2(ii)(*b*), that in the rhombus reduces from C_s to C_1 as in Fig. 2(ii)(*a*). Thus, the second octagonal QP pattern can be determined uniquely.

In the DPQT case, the point group of the inflated o.a. patterns of rhombus C_{2v} and triangle C_s are reduced to the lower C_1, but that of the square C_s is conserved as in Fig. 2(ii)(*c*). In the polar case, the inflated pattern could not be determined uniquely by only the arrow on the edges but this problem is resolved by considering the inflated pattern of the o.a. of the base tiles.

It is shown that, after all, the matching rule in both cases results in the orientation of the inflated pattern, consequently the arrow notation should be presented on the tile surfaces rather than on the tile edges.

4. Inflation transformation of DQPT

In this section, the properties of the DQPT pattern are discussed. As shown in the previous section, DQPT is composed of three kinds of base tile: rhombus, regular triangle and square. If $R^{(0)}$, $T^{(0)}$ and $S^{(0)}$ represent the zeroth-generation tiles, respectively, the area of each base tile is given by $|R^{(0)}|=\frac{1}{2}$, $|T^{(0)}|=3^{1/2}/4$ and $|S^{(0)}|=1$, respectively. The first generation of the inflated rhombus

consists of three $R^{(0)}$, eight $T^{(0)}$ and two $S^{(0)}$; the regular triangle of two $R^{(0)}$, seven $T^{(0)}$ and two $S^{(0)}$; and the square of six $R^{(0)}$, sixteen $T^{(0)}$ and four $S^{(0)}$. The self-similar transformation matrix $\mathbf{M}$ is represented as follows:

$$\mathbf{M} = \begin{pmatrix} 3 & 8 & 2 \\ 2 & 7 & 2 \\ 6 & 16 & 4 \end{pmatrix}. \tag{1}$$

Here, three eigenvalues of $\mathbf{M}$, $\sigma_1 = 7 + 4 \times 3^{1/2}$, $\sigma_2 = 7 - 4 \times 3^{1/2}$ and $\sigma_3 = 0$, are obtained taking into account the singularity of $\mathbf{M}$ (the third row is twice the first row). The value of $\sigma_1 = 7 + 4 \times 3^{1/2}$ corresponds to the square of the inflation scale of base vector $2 + 3^{1/2}$, so that σ_1 is the inflation scale of the area of the constituent tile. The relation $\sigma_2 = 1/\sigma_1$ shows that the two eigenvalues take the inflation and deflation scales, respectively. Zero σ_3 eigenvalue means there exists one tile that is represented by a linear combination of the other two tiles. In this case, the condition $|S^{(n)}| = 2|R^{(n)}|$ is taken into account for the following diagonalization of $\mathbf{M}$.

Let $\mathbf{U}^{(0)}$ be the column vector of a set of areas of base tiles of DQPT:

$$\mathbf{U}^{(0)} = \begin{pmatrix} |R^{(0)}| \\ |T^{(0)}| \\ |S^{(0)}| \end{pmatrix}, \tag{2}$$

then the nth-generation column vector $\mathbf{U}^{(n)}$ is represented as

$$\mathbf{U}^{(n)} = \mathbf{M}\mathbf{U}^{(n-1)} = \mathbf{M}^2\mathbf{U}^{(n-2)} = \ldots = \mathbf{M}^n\mathbf{U}^{(0)}. \tag{3}$$

Consequently, quasiperiodicity is proved using an expanded form of $\mathbf{M}^n$. The ratios of the numbers of base tiles should converge to an irrational number when n approaches infinity.

In order to determine the nth power of such an inflation matrix $\mathbf{M}^n$, matrices $\mathbf{T}$ and $\mathbf{T}^{-1}$ are introduced as follows:

$$\mathbf{T} = \begin{pmatrix} 1 & 0 & 0 \\ 0 & 1 & 0 \\ 2 & 0 & 1 \end{pmatrix}, \quad \mathbf{T}^{-1} = \begin{pmatrix} 1 & 0 & 0 \\ 0 & 1 & 0 \\ -2 & 0 & 1 \end{pmatrix}, \tag{4}$$

where $\mathbf{T}\mathbf{T}^{-1} = \mathbf{I}$ (unit matrix). In order to diagonalize $\mathbf{M}$, a similar transformation of $\mathbf{M}$ is presented:

$$\tilde{\mathbf{M}} = \mathbf{T}^{-1}\mathbf{M}\mathbf{T}, \quad \tilde{\mathbf{M}}^2 = \mathbf{T}^{-1}\mathbf{M}^2\mathbf{T}, \quad \ldots, \quad \tilde{\mathbf{M}}^n = \mathbf{T}^{-1}\mathbf{M}^n\mathbf{T} \tag{5}$$

or

$$\mathbf{M}^n = \mathbf{T}\tilde{\mathbf{M}}^n\mathbf{T}^{-1}. \tag{6}$$

Here, all the third-row elements of $\tilde{\mathbf{M}}$ are zero and the first- and second-row elements of $\tilde{\mathbf{M}}$ are partitioned into a 2×2 matrix $\hat{\mathbf{M}}$ and a column matrix $\begin{pmatrix} \hat{m}_{13} \\ \hat{m}_{23} \end{pmatrix}$. Thus, $\tilde{\mathbf{M}}$ is represented by $\hat{\mathbf{M}}$ and $\begin{pmatrix} \hat{m}_{13} \\ \hat{m}_{23} \end{pmatrix}$ as follows.

$$\tilde{\mathbf{M}} = \begin{pmatrix} & \hat{\mathbf{M}} & & \begin{pmatrix} \hat{m}_{13} \\ \hat{m}_{23} \end{pmatrix} \\ 0 & & 0 & 0 \end{pmatrix}. \tag{7}$$

Here,

$$\hat{\mathbf{M}} = \begin{pmatrix} \hat{m}_{11} & \hat{m}_{12} \\ \hat{m}_{21} & \hat{m}_{22} \end{pmatrix} = \begin{pmatrix} 7 & 8 \\ 6 & 7 \end{pmatrix}, \quad \begin{pmatrix} \hat{m}_{13} \\ \hat{m}_{23} \end{pmatrix} = \begin{pmatrix} 2 \\ 2 \end{pmatrix}. \tag{8}$$

From successive calculation of (5) for $n = 1, 2, 3, \ldots$, the nth-generation matrix form of $\tilde{\mathbf{M}}^n$ is deduced:

$$\tilde{\mathbf{M}}^n = \begin{pmatrix} & \hat{\mathbf{M}}^n & & \hat{\mathbf{M}}^{(n-1)}\begin{pmatrix} \hat{m}_{13} \\ \hat{m}_{23} \end{pmatrix} \\ 0 & & 0 & 0 \end{pmatrix}. \tag{9}$$

Equation (9) is confirmed by the mathematical induction as follows.

$$\tilde{\mathbf{M}}\tilde{\mathbf{M}}^n = \tilde{\mathbf{M}}^{(n+1)} = \begin{pmatrix} & \hat{\mathbf{M}}^{(n+1)} & & \hat{\mathbf{M}}^n\begin{pmatrix} \hat{m}_{13} \\ \hat{m}_{23} \end{pmatrix} \\ 0 & & 0 & 0 \end{pmatrix}. \tag{10}$$

$\mathbf{M}^n$ is obtained by substituting (9) into (6). The expanded form of $\mathbf{M}^n$ is determined by $\hat{\mathbf{M}}^n$ and $\hat{\mathbf{M}}^{(n-1)}$. Since the eigenvalues of $\hat{\mathbf{M}}$ are $\sigma_+ = (7 + 4 \times 3^{1/2})/2$ and $\sigma_- = (7 - 4 \times 3^{1/2})/2$, $\hat{\mathbf{M}}^n$ is represented, by calculation of the usual diagonalization, as

$$\hat{\mathbf{M}}^n = \begin{pmatrix} 2^{(n-1)}(\sigma_+^n + \sigma_-^n) & (2^n \times 3^{1/2}/3)(\sigma_+^n - \sigma_-^n) \\ 2^{(n-2)}3^{1/2}(\sigma_+^n - \sigma_-^n) & 2^{(n-1)}(\sigma_+^n + \sigma_-^n) \end{pmatrix}. \tag{11}$$

$\tilde{\mathbf{M}}^n$ is determined by substitution of $\hat{\mathbf{M}}^n$ and $\hat{\mathbf{M}}^{(n-1)}$ into those in (9) and consequently $\mathbf{M}^n$ is obtained using (6). The matrix elements of $\mathbf{M}^n(m_{ij})$ are represented with σ_+ and σ_- as follows.

$$\begin{aligned} m_{11} &= (2^{n-1}/3)\{(\sigma_+ + 1)\sigma_+^{n-1} + (\sigma_- + 1)\sigma_-^{n-1}\} \\ m_{12} &= (3^{1/2} \times 2^n/3)\{(\sigma_+^n - \sigma_-^n)\} \\ m_{13} &= (2^{n-1}/3)\{(\sigma_+ - \tfrac{1}{2})\sigma_+^{n-1} + (\sigma_- - \tfrac{1}{2})\sigma_-^{n-1}\} \\ m_{21} &= 3 \times 2^{n-4}\{(\sigma_+ - \tfrac{5}{6})\sigma_+^{n-1} + (\sigma_- - \tfrac{5}{6})\sigma_-^{n-1}\} \\ m_{22} &= 2^{n-1}(\sigma_+^n + \sigma_-^n) \\ m_{23} &= 2^{n-3}\{(\sigma_+ + \tfrac{1}{2})\sigma_+^{n-1} + (\sigma_- + \tfrac{1}{2})\sigma_-^{n-1}\} \\ m_{31} &= 2m_{11}, \quad m_{32} = 2m_{12}, \quad m_{33} = 2m_{13}. \end{aligned} \tag{12}$$

5. Convergence of occurrence frequency of $\mathbf{U}^{(n)}$

The estimation of the occurrence frequency of the base tiles in $R^{(n)}$, $T^{(n)}$ and $S^{(n)}$ when n approaches ∞ is considered based on (3). The frequency of each tile is represented in the form of the ratios of numbers of each

base tile in every inflated tile, *i.e.*

$$\begin{array}{llll} m_{12}/m_{11}, & m_{13}/m_{11}, & m_{13}/m_{12} & \text{in } R^{(n)}, \\ m_{22}/m_{21}, & m_{23}/m_{21}, & m_{23}/m_{22} & \text{in } T^{(n)}, \\ m_{32}/m_{31}, & m_{33}/m_{31}, & m_{33}/m_{32} & \text{in } S^{(n)}. \end{array} \tag{13}$$

It is obvious from (12) that the ratios of numbers in $S^{(n)}$ have the same values as in $R^{(n)}$; consequently, the calculation is carried out only for the ratios in $R^{(n)}$ and $T^{(n)}$. The ratios of numbers of two kinds of base tiles in different inflated tiles should converge to the same limiting value of irrational number when the size of an inflated tile becomes infinite by the self-similar operation. The calculation of these ratios is carried out using (12). The convergent values for infinite n are presented as follows.

$$\begin{aligned} n \to \infty \quad & m_{12}/m_{11} = m_{22}/m_{21} = m_{32}/m_{31} \\ & \to (16 + 10 \times 3^{1/2})/11 \\ n \to \infty \quad & m_{13}/m_{11} = m_{23}/m_{21} = m_{33}/m_{31} \\ & \to (2 + 4 \times 3^{1/2})/11 \\ n \to \infty \quad & m_{13}/m_{12} = m_{23}/m_{22} = m_{33}/m_{32} \to 2 - 3^{1/2}. \end{aligned} \tag{14}$$

The necessary condition of quasiperiodicity is verified by the existence of an irrational number of convergent values in (14).

6. Concluding remarks

A new quasiperiodic pattern with dodecagonal symmetry is presented by self-similar inflation. Properties of DQPT, the quasiperiodicity of the pattern and the fractal dimension of the boundary are investigated. This pattern is characterized and determined uniquely by the inflation rule which depends on the orientation of the base tiles in the first-generation tile.

Another interest of DQPT is the classification of the types of vertex where three kinds of tile assemble and their convergent values of occurrence frequency in the infinite tile. These problems will be discussed elsewhere with those of fractal growth of each tile or the acceptance domain.

The authors thank Professor Tateaki Sasaki of Tsukuba University for valuable discussions on the algebraic treatment and Mr Ikegami of Instrumentation and Characterization Center and the staff of the Computation Center, both of the Institute of Physical and Chemical Research, for technical support and drawing figures.

This work is partly supported by Special Coordination Funds for Promoting Science and Technology.

References

BEENKER, F. P. M. (1982). TH Report 82-WSK-04. Eindhoven Technical Univ., The Netherlands.

BRUIJN, N. G. DE (1981). *Proc. K. Ned. Akad. Wet. Ser. A*, **84**, 39–52, 53–66.

FUNG, K. K., YANG, C. Y., ZHOU, Y. Q., ZHAO, J. G., ZHAN, W. S. & SHEN, B. G. (1986). *Phys. Rev. Lett.* **56**, 2060–2063.

ISHIMASA, T., NISSEN, H. U. & FUKANO, Y. (1985). *Phys. Rev. Lett.* **55**, 511–513.

LÜCK, R. (1993). *Int. J. Mod. Phys.* B7, 1437–1453.

MANDELBROT, B. B. (1983). *The Fractal Geometry of Nature*, pp. 36–44. New York: Freeman.

NIIZEKI, K. & MITANI, H. (1987). *J. Phys. A: Math. Gen.* **20**, L405–L410.

SHECHTMAN, D., BLECH, I., GRATIAS, D. & CAHN, J. W. (1984). *Phys. Rev. Lett.* **53**, 1951–1953.

SOCOLAR, J. E. S. (1989). *Phys. Rev.* B**39**, 10519–10551.

STAMPFLI, P. (1986). *Helv. Phys. Acta*, **59**, 1260–1263.

WATANABE, Y. & IKEGAMI, Y. (1991). *Proceedings of China–Japan Seminars QUASICRYSTALS*, pp. 204–211. Singapore: World Scientific.

WATANABE, Y., ITO, M. & SOMA, T. (1987). *Acta Cryst.* A**43**, 133–134.

WHITTAKER, E. J. W. & WHITTAKER, R. M. (1988). *Acta Cryst.* A**44**, 105–112.

YANG, Q. B. & WEI, W. D. (1987). *Phys. Rev. Lett.* **58**, 1020–1022.

ZOBETZ, E. (1992). *Acta Cryst.* A**48**, 328–335.

ZOBETZ, E. & PREISINGER, A. (1990). *Acta Cryst.* A**46**, 962–969.